Journal of Electronic Imaging

JElectronicImaging.org

Infrared small target detection method based on decomposition of polarization information

Yan Zhang
Zhi-Guang Shi
Tiao-Wen Qiu

SPIE. IS&T imaging.org

Yan Zhang, Zhi-Guang Shi, Tiao-Wen Qiu, "Infrared small target detection method based on decomposition of polarization information," *J. Electron. Imaging* **26**(3), 033004 (2017), doi: 10.1117/1.JEI.26.3.033004.

Infrared small target detection method based on decomposition of polarization information

Yan Zhang,* Zhi-Guang Shi, and Tiao-Wen Qiu
National University of Defense Technology, ATR Key Laboratory of the School of Electronic Science and Engineering, Changsha, China

Abstract. A method of feature extraction and small target detection, based on infrared polarization, which uses the technical superiority of infrared polarization imaging in artificial target detection to solve the clutter interference problem in infrared target detection, is proposed. First, using the differences in the polarization characteristics of the artificial target and the natural background, the infrared polarization information models for the target and background are established. The compositions of intensity information, polarization information, and target polarization information are extracted, and enhancement measures are analyzed. Then, the variable polarization theories are combined to extract the target polarization characteristics and suppress the background clutter. Finally, the infrared small target is detected, and comparisons with existing methods demonstrate the effectiveness and reliability of the proposed method. [DOI: 10.1117/1.JEI.26.3.033004]

Keywords: small target detection; infrared polarization information; feature extraction; variable polarization; Stokes vector; modeling.

Paper 161016 received Dec. 6, 2016; accepted for publication Apr. 14, 2017; published online May 10, 2017.

1 Introduction

Infrared small target detection is important in antimissile and air-defense applications, early warning and reconnaissance systems, air strikes, and other such fields. Because of background clutter and noise interference in infrared detector imaging planes, small targets occupying few pixels are often drowned in clutter or noise. Thus, small target detection is a difficult problem. With the introduction of infrared camouflage stealth and infrared decoy technologies, the traditional target detection methods based on infrared radiation intensity imaging are facing great challenges. In the past decade, infrared polarization imaging detection technology has been further developed for multiple applications. The technology not only detects the infrared radiation intensity information from the target scene, it can also obtain the polarization information of the infrared radiation, as well as differentiate targets with the same infrared radiation intensity, based on their polarization characteristics, such as the degree of polarization, the polarization angle, the difference between the horizontal and vertical polarization components, the difference between the 45-deg and 135-deg polarization components, and so on. Because of the above characteristics and advantages, the infrared polarization imaging detection technology has become an effective method to solve the problems in man-made target detection.

Since 1960, scholars have been conducting exploratory studies on infrared polarization and since then, have progressed to target detection and recognition. Tooley[1] investigated the feasibility of artificial target detection using infrared polarization information and proposed the method of restraining the background using the differences between the horizontal polarization component and the vertical polarization component, to implement target detection. Sadjadi and Chun[2] extracted statistical features of the target using the infrared radiation intensity, degree of polarization, and three-channel information of the polarization angle and used them as the basis to achieve small target detection. In 2003, the same research team[3] addressed the problem of detecting small military targets on the ground by means of an autonomous polarimetric sensor on board a high-altitude airborne or space-borne platform. Romano et al.[4] presented an anomaly detection algorithm based on long-wave infrared polarization imaging and the Bayes decision to achieve all day and night man-made target detection. Yang et al.[5] first employed the mean-shift algorithm to aggregate the infrared and polarized images, and then used the Dempster–Shafer evidence theory to fuse the object information from the clustered infrared and polarized images for target detection. Mogen et al.[6] used morphological filters to enhance the similarities in the background and then regarded the Q image as a low-rank matrix and the small target as redundant data that disrupted the similarity in the background. They then used the stable recovery matrix to build a background-suppression mathematical model. Although these methods can detect artificial targets in complex backgrounds by using polarization information, their clutter and noise suppression abilities can be improved if the polarization difference mechanism is explored more thoroughly.

While studying the infrared polarization principle and polarization imaging mechanisms, we find that the polarization state of the target scene is often partially polarized and can be decomposed into a sum of linearly polarized components and natural light components; if the natural light components can be decomposed and a sum of linearly polarized components can be extracted, target detection and segmentation can be achieved. Based on this idea, a target detection method using the infrared polarization information is proposed in this paper. Once the infrared polarization information model is established, the Stokes vector, the vector decomposition of partially polarized light, and the variable polarization theory are combined to realize background

*Address all correspondence to: Yan Zhang, E-mail: atrthreefire@nudt.edu.cn

clutter suppression, random noise elimination, and target polarization characteristic enhancement. Thus, an infrared small target can be detected. Simulations demonstrate the effectiveness and reliability of this proposed method.

2 Basic Scheme

2.1 *Infrared Polarization Information Modeling*

The infrared radiation from the target scene, a light wave treated as partially polarized light, is composed by the superposition of polarized and unpolarized light; unpolarized light is also known as natural light.[7] After entering the imaging detection device, the infrared radiation from the object scene is converted to an infrared image, and the radiation intensity becomes the grayscale value of the image. The corresponding natural light component is denoted by I_N and the linearly polarized light component is denoted by I_P. Since we are dealing with passive imagery, one can ignore the circularly polarized components; therefore, the radiation intensity can be decomposed into

$$I = I_N + I_P. \tag{1}$$

If polarization component extraction was to be performed on the radiation intensity I, according to the Marius (E. L. Malus) law,[8] the intensity of the polarization component extracted in the polarization direction θ would be

$$I^\theta = I_N^\theta + I_P^\theta = \frac{1}{2} I_N + I_P \cos^2(\theta - A), \tag{2}$$

with a natural light component $I_N^\theta = \frac{1}{2} I_N$ and a linear-polarization component $I_P^\theta = I_P \cos^2(\theta - A)$, where A is the polarization angle defined as the angle between the polarization direction of incident light and the reference direction of the x-axis.

According to the defined formula for the degree of polarization

$$\mathrm{Dop} = \frac{|I_{\text{II}} - I_\perp|}{I_{\text{II}} + I_\perp}, \tag{3}$$

where I_{II} and $I_\perp$ are the polarization component intensities of two mutually perpendicular polarization components.

By considering I_{II} as the polarization component intensity in the direction of the polarization angle A, from Eq. (2), we obtain

$$I_{\text{II}} = I^A = I_N^A + I_P^A = \frac{1}{2} I_N + I_P, \tag{4}$$

where $I_\perp$ is the polarization component intensity in the direction perpendicular to I_{II}; therefore, from Eq. (2), we obtain

$$I_\perp = I^{A+\frac{\pi}{2}} = I_N^{A+\frac{\pi}{2}} + I_P^{A+\frac{\pi}{2}} = \frac{1}{2} I_N. \tag{5}$$

From Eqs. (3)–(5), we obtain the degree of polarization of the target pixels and background pixels

$$P = \frac{I_P}{I_N + I_P} = \frac{I_P}{I}. \tag{6}$$

For infrared polarization images obtained in an arbitrary polarization direction θ, the grayscale values of the target and background pixels are defined as follows:

$$\begin{cases} I_T^\theta(i,j) = I_{TN}^\theta(i,j) + I_{TP}^\theta(i,j) + w & (i,j) \in \text{target} \\ I_B^\theta(i,j) = I_{BN}^\theta(i,j) + I_{BP}^\theta(i,j) + w & (i,j) \in \text{background} \end{cases}. \tag{7}$$

In the first formula in the above equation, $I_T^\theta(i,j)$ is the polarized light intensity of the target pixels in the polarization direction θ, $I_{TN}^\theta(i,j)$ is the natural light component of the target pixels, $I_{TP}^\theta(i,j)$ is the linearly polarized component of the target pixels, and ω is the pixel noise. Similarly, the terms in the second formula are the corresponding parameters for the background pixels.

Combining Eqs. (2), (6), and (7), we obtain the infrared polarization information model as follows:

$$\begin{cases} I_T^\theta(i,j) = I_T(i,j)\left\{\frac{1}{2}[1 - P_T(i,j)] + P_T(i,j)\cos^2[\theta - A_T(i,j)]\right\} + w & (i,j) \in \text{target} \\ I_B^\theta(i,j) = I_B(i,j)\left\{\frac{1}{2}[1 - P_B(i,j)] + P_B(i,j)\cos^2[\theta - A_B(i,j)]\right\} w & (i,j) \in \text{background} \end{cases}. \tag{8}$$

In the above equation, $I_T(i,j)$ and $I_B(i,j)$ are the infrared intensity values of target and background pixels, respectively. In the model, the intensity information and polarization information (degree of polarization and polarization angle) are expressed as two multiplication factors.

2.2 *Polarization Information Decomposition Principle*

In Eq. (8), without considering the noise ω, the change curves of the infrared polarization intensities of the target and background pixels in the polarization direction θ form an ellipse. The ellipticity of the ellipse is the degree of polarization P, the long-axis direction of the ellipse is the direction of the polarization angle A, and the inscribed circle in the ellipse is the natural light composition. It is thus clear that the polarized radiation intensity is composed of natural light components and linearly polarized components. The linearly polarized light component in the direction of the polarization angle is the largest, and the linearly polarized component in the direction perpendicular to the polarization angle is the least, as shown in Fig. 1.

As shown in Fig. 1, due to the difference between the background polarization angle and the target polarization angle, if we calculate the polarized light intensity in a direction perpendicular to the background polarization angular direction, we obtain a polarization intensity map $I^{\bar{A}-\pi/2}$. This map contains the partially polarized light objects and the natural light background, which is the linearly polarized light component without the background. In the actual processing, the background polarization angle direction can be replaced by the average value $\bar{A}$ of the entire polarization angle image.

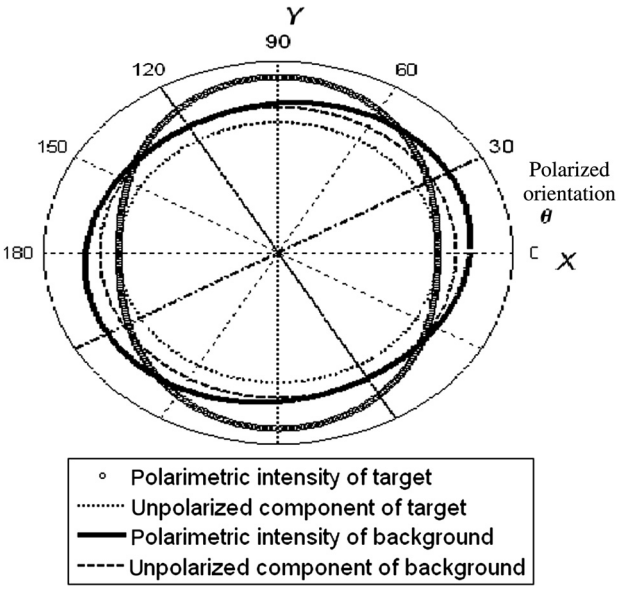

Fig. 1 Variation curves of polarized light intensities of target and background with a polarization direction θ.

Therefore, the basic concept of the method can be summarized as follows: first, based on the difference between the target polarization angle and the background polarization angle, the full polarization direction optimization method[9] is used to retain as much target polarization information as possible while eliminating as much background polarization information as possible. For a small target taking up a small amount of pixels, the average value of the background polarization angle ($\overline{A_B} \approx \bar{A}$) can be approximated using the polarization angle mean of the whole image and then calculating the variable polarization component $I^{\bar{A}-\pi/2}$ in the direction perpendicular to background polarization angle. Thus, the completely polarized components in the background can be eliminated, and the completely polarized components in the target can be retained.

For a point target submerged in a background with strong clutter light, most of the intensity information cannot be used for identifying the target and background. Therefore, using the decomposition of the completely polarized component, the natural light component $I_N^{\bar{A}-\pi/2} = \frac{1}{2} I_N$ in the polarized component $I^{\bar{A}-\pi/2}$ can be removed. Thus, the background information can be completely suppressed, retaining only the completely polarized component $I_{TP}^{\bar{A}-\pi/2}$ of the target, as in Eq. (9), and the target polarization feature extraction achieved through the threshold can complete the target detection. The value of the threshold could refer to Ref. 7. Figure 2 shows the schematic diagram of the principle of the proposed method

$$I_{TP}^{\bar{A}-\pi/2} = I^{\bar{A}-\pi/2} - \frac{1}{2} I_N. \tag{9}$$

3 Implementation Process

A set of polarimetric image that had at least three polarization directions is fed to the algorithm (Fig. 3). The process is as follows:

1. Polarization state calculation for target scene: Arbitrary infrared polarized light can be expressed using the Stokes vector. After acquiring the polarized light intensity (I^{θ_1}, I^{θ_2}, and I^{θ_3}) in more than three polarization directions, we can calculate each Stokes parameter I, Q, and U using Eq. (10). The target scene polarization state S is calculated, and the degree of polarization P[9] and the polarization angle A[9] are calculated

$$I^{\theta} = I' \frac{1}{2}(I + Q \cos 2\theta + U \sin 2\theta). \tag{10}$$

2. Polarization state decomposition for target scene: The polarization state of the target scene is often partially polarized and can be decomposed into a sum of linearly polarized components and natural light components. Thus, we obtain the linearly polarized light component intensity $I_P = \sqrt{Q^2 + U^2 + V^2}$ and the natural light component intensity $I_N = I - \sqrt{Q^2 + U^2 + V^2}$.
3. Calculate the variable polarization component $I^{\bar{A}-\pi/2}$: By considering the polarization direction θ as $\bar{A} - \pi/2$, the variable polarization component $I^{\bar{A}-\pi/2}$ can be obtained perpendicular to the direction of the average value of the polarization angle A using Eq. (10). Thereby, the linearly polarized light component $I_{BP}^{\bar{A}-\pi/2}$ of the background pixels is suppressed.

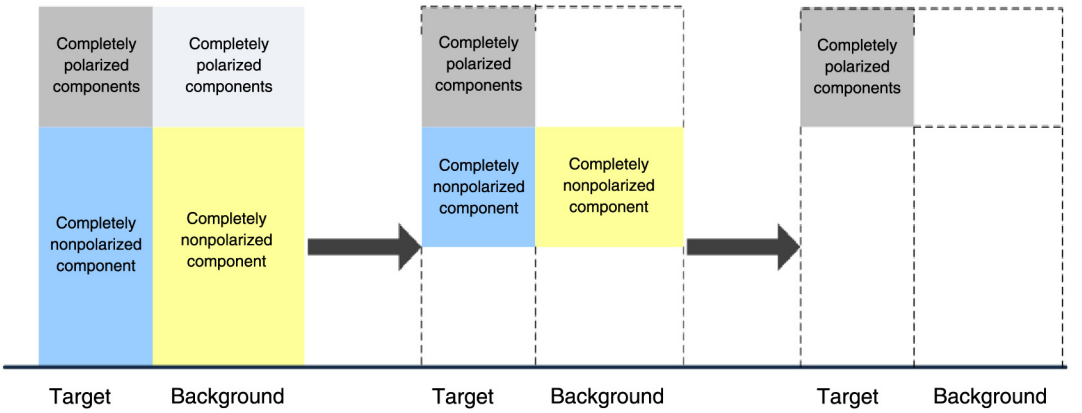

Fig. 2 Schematic diagram of point target detection principle based on decomposition of polarization information.

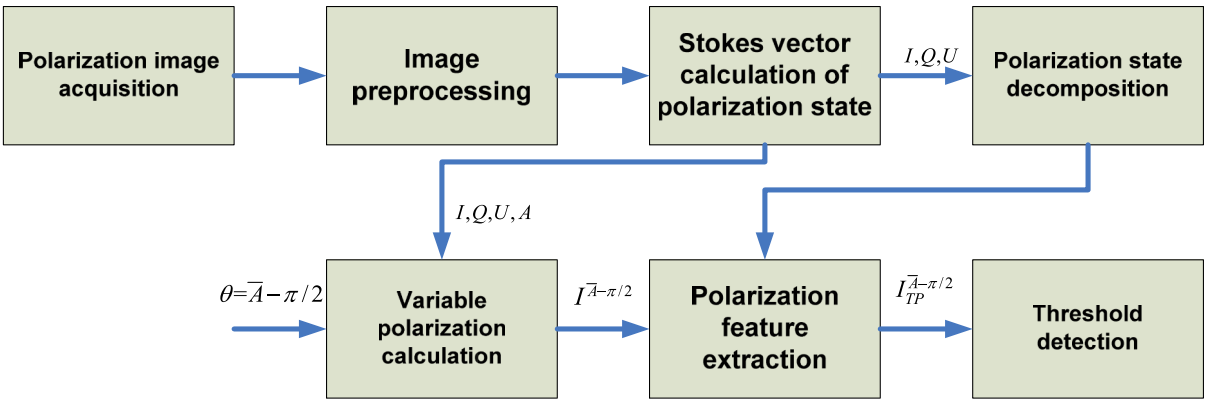

Fig. 3 Flow chart of small target detection algorithm.

4. Linearly polarized light component extraction from the variable polarization component: Using the calculated results from the above two steps [Eqs. (4) and (5)], we remove the natural light polarization component $I_N^{\bar{A}-\pi/2} = \frac{1}{2} I_N$ from the variable polarization component $I^{\bar{A}-\pi/2}$, retaining the linearly polarized light component $I_{TP}^{\bar{A}-\pi/2}$ of the target pixels.
5. Complete small target detection: Conduct threshold[10] detection using a suitable threshold $I_{TP}^{\bar{A}-\pi/2}$.

4 Results and Analysis of Simulation Experiments

4.1 *Experimental Results and Analysis of Algorithm*

A set of target image data is used to verify the effectiveness of the proposed algorithm in our long-wave infrared polarization detection system, and the system consists of four parts: mechanical rotary polarizer, long-wave infrared detector, image data acquisition device, and information processing system. The mechanical rotary polarizer can obtain the data from 0 to 360 angle polarized image. This set of image data includes the original infrared image, 0 deg, 45 deg, and 135 deg three polarization direction of the infrared polarized image. The image is composed of the target and a 640×512 background with clutter and random noises, as shown in Fig. 4.

According to the Stokes vector polarization characteristics method,[11] the polarization characteristic parameters, such as I, Q, and U, the degree of polarization P, and the polarization angle A are calculated, and the corresponding images are shown in Fig. 5. The target is still embedded in strong background clutter. The background clutter in image P and image A is very strong; however, A is more sensitive to noise sources.

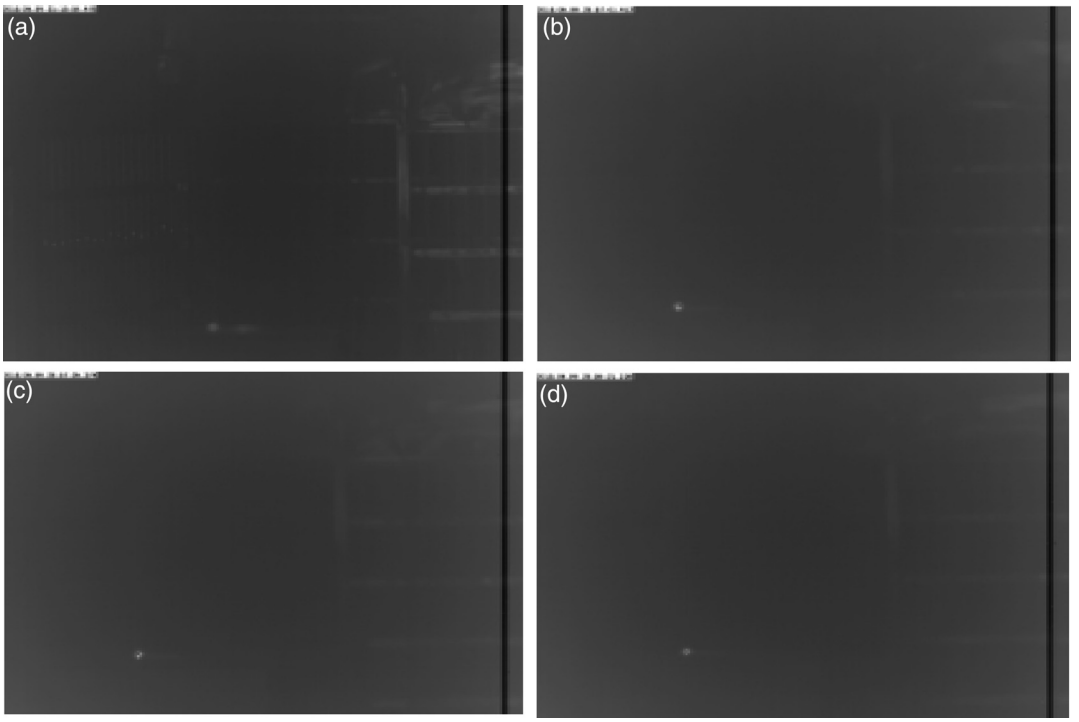

Fig. 4 The infrared intensity image and the polarization images: (a) original intensity image, (b) image with a polarization direction of 0 deg, (c) image with a polarization direction of 45 deg, and (d) image with a polarization direction of 135 deg.

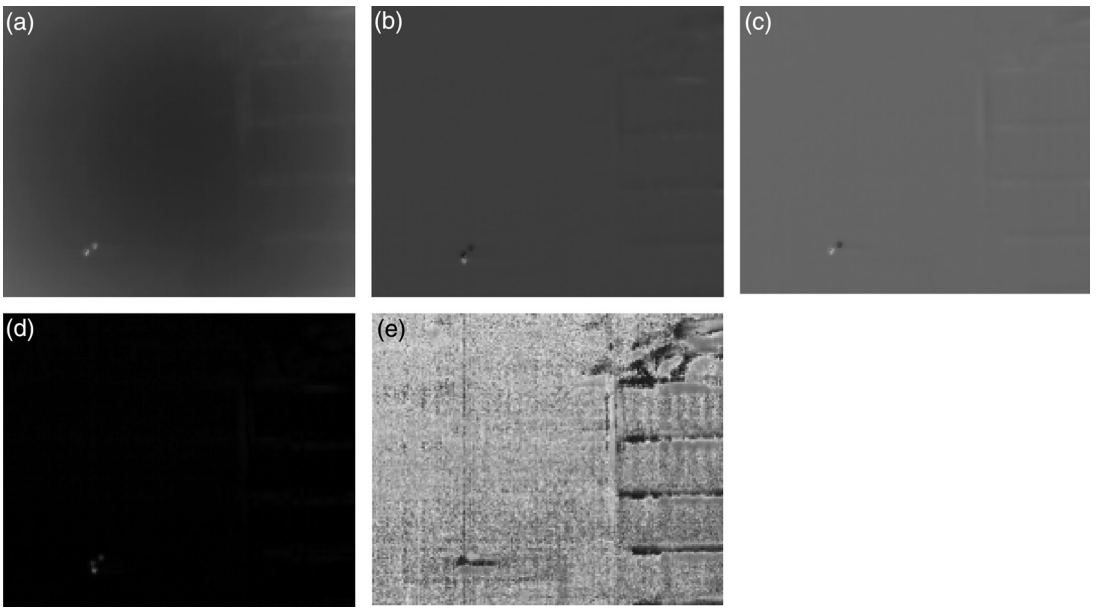

Fig. 5 (a) Image of I, (b) image of Q, (c) image of U, (d) image P of the degree of polarization, and (e) image A of the polarization angle.

Fig. 6 Images of detection results: (a) variable polarization image $I^{\bar{A}-\pi/2}$, (b) resulting image after processing using the algorithm $I_{TP}^{\bar{A}-\pi/2}$, and (c) resulting image after threshold segmentation.

In Fig. 6, the left image is the variable polarization image $I^{\bar{A}-\pi/2}$ perpendicular to the mean value direction of the polarization angle, from which the natural light component is removed and the linearly polarized light component of variable polarization $I_{TP}^{\bar{A}-\pi/2}$ is obtained. The background clutter has been largely suppressed making it easy to detect the small target.

For each of the above images, two parameters—the contrast C between the target and background, and the local signal-to-noise ratio (SNR) LSC[9]—are used to evaluate the effectiveness of the detection algorithm. C reflects the prominence degree of the target signal in the background clutter and LSCR reflects the state of noise suppression, defined as

$$C = \left| \frac{\mu_T - \mu_B}{\mu_T + \mu_B} \right|, \tag{11}$$

$$\mathrm{LSCR} = \left| \frac{\mu_T - \mu_B}{\sigma_B} \right|. \tag{12}$$

The contrast C between the target and the background, and the local SNR LSCR of each parameter are calculated as shown in Table 1. The results show that the image parameters increased significantly after processing using the proposed method and that they are significantly greater than the other parameter values. Thus, background clutter noise is suppressed effectively highlighting the target in the scene.

4.2 *Comparison and Analysis Using Existing Methods*

To measure the performance of the detection method further, the method is compared with three existing methods in Refs. 1–3; the detection results of the four methods are shown in Fig. 7. It is clear that the proposed method can achieve better background suppression and noise elimination. The method in Ref. 1 cannot eliminate the random noise thoroughly, the method in Ref. 2 fails to suppress the background effectively, and the method in Ref. 3 is sensitive to the undulations in the background and cannot effectively distinguish between real and false targets.

To quantitatively compare the performances of the four methods, the C and LSCR values are used to evaluate the detection speeds based on the program running time (hardware environment: Intel G630 2.70-GHz CPU, 1.84-GB memory and software: Windows XP and MATLAB® R2013 platform). The time of image input and preprocessing is not included, only the running time of the detection algorithm is

Table 1 C values and LSCR values of each parameter image.

Parameter	Original intensity image	$I^{0\ deg}$	$I^{45\ deg}$	$I^{135\ deg}$	I	Q
C	0.0904	0.0801	0.0831	0.0829	0.0827	6.3469×10^{-4}
LSCR	0.6663	0.6852	0.6220	06983	0.8113	0.8607
Parameter	U	P	A	$I^{\tilde{A}-\pi/2}$	$I_{TP}^{\tilde{A}-\pi/2}$	
C	5.857×10^{-4}	Target not detected	Target not detected	0. 5320	1	
LSCR	0.8945	Target not detected	Target not detected	0.9625	0.9813	

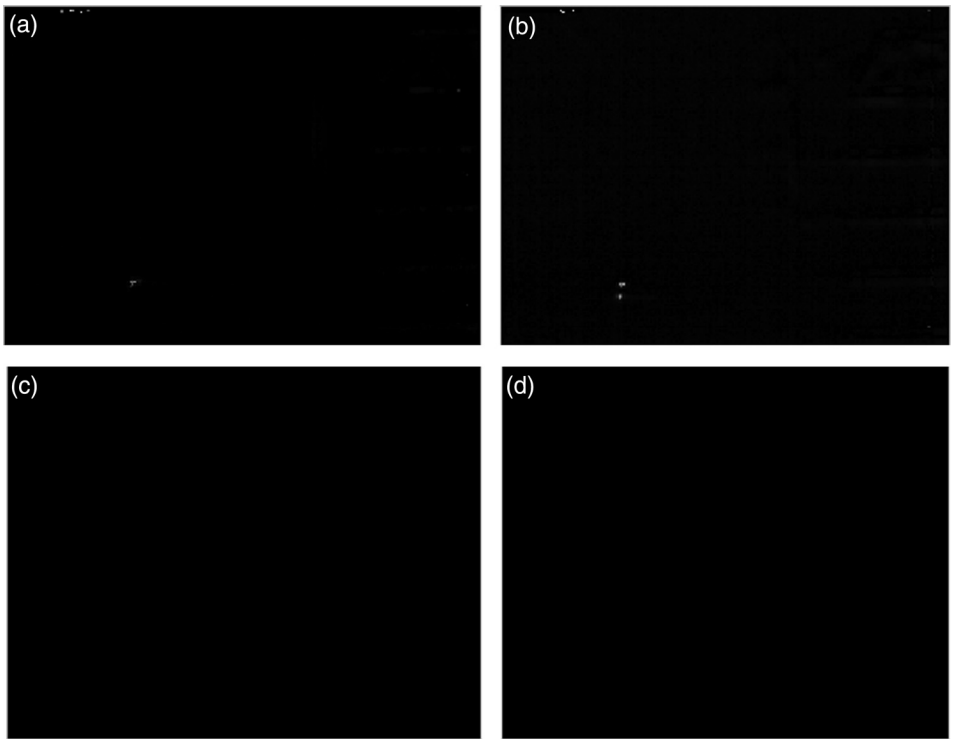

Fig. 7 Comparison of the resulting images of four methods: (a) detection result of the method proposed in this paper, (b) detection result of the method in Ref. 1, (c) detection result of the method in Ref. 2, and (d) detection results of the method in Ref. 3.

calculated. The results are shown in Table 2. The C and LSCR of the proposed method are obviously higher than that of the other methods, and the running time is relatively shorter, which indicates that the proposed method is better than the three existing methods and is consistent with the above subjective evaluation.

Table 2 Performance comparison of four detection methods.

	Our method	Method in Ref. 1	Method in Ref. 2	Method in Ref. 3
C	1	0. 3650	Target not detected	Target not detected
LSCR	0.9813	0.9355	Target not detected	Target not detected
Running time/s	0.263559	0.35829	4.223324	4.607037

5 Conclusion

A method based on the differences in the infrared polarization characteristics of an artificial target and its natural background, such as the distribution differences in the degree of polarization or polarization angle, was proposed. According to the existing research results, the degree of polarization of the artificial target is greater than that of the natural background. The distribution of the degree of polarization of the artificial target is more concentrated than that of the natural background, and the polarization angle of the man-made target is quite different from that of the natural background. Therefore, the theoretical basis of the experiments is reliable. Even subtle differences in the degree of polarization are useful, and in the case where the degrees of polarization of the target and the background are similar, the proposed method can still be utilized as it can use the differences in the polarization angles. In practice, the double difference—the degree of polarization and the polarization angle—between the

target and the background provides abundant information, which increases the reliability of the method. The infrared polarization data containing small target, background clutter were used for the experiments and analysis of this method, and the experimental results showed that the method could suppress the background clutter and noise well and highlight the target information. The comparisons with three existing methods for detection also reflected the effectiveness, reliability, and simplicity of the proposed method.

Acknowledgments

This paper was supported by the National Natural Science Foundation of China under fund No. 61302145.

References

1. R. D. Tooley, "Man-made target detection using infrared polarization," *Proc. SPIE* **1166**, 52 (1990).
2. F. A. Sadjadi and C. S. L. Chun, "New experiments in the use of infrared polarization in the detection of small targets," *Proc. SPIE* **4379**, 144 (2001).
3. F. A. Sadjadi and C. S. L. Chun, "Automatic detection of small objects from their infrared state-of-polarization vectors," *Opt. Lett.* **28**, 531–533 (2003).
4. J. M. Romano, D. Rosario, and J. McCarthy, "Day/night polarimetric anomaly detection using SPICE imagery," *IEEE Trans. Geosci. Remote Sens.* **50**(12), 5014–5023 (2012).
5. W. Yang et al., "Method of target detection for infrared polarization image," *Infrared Laser Eng.* **43**(8), 2746–2751 (2014).
6. X. Mogen et al., "Research of desert infrared polarization dim and small target detection method," *Acta Photonica Sin.* **43**(10), 1010003 (2014).
7. H. Long, Z. Zhang, and H. Tan, *The Polarization of Light and Its Application*, Mechanical Industry Press, Beijing (1999).
8. M. von Rohr, *Geometrical Investigation of the Formation of Images in Optical Instruments*, p. 21, M.M. Stationary, London (1920).
9. G. Cheng et al., "Infrared dim small target detection based on morphological band-pass filtering and scale space theory," *Acta Opt. Sin.* **32**(10), 1015001 (2012).
10. Y. Zhang, Z. Shen, and P. Wang, "Background estimation and the infrared small target detection based on RBF neural network," *J. Natl. Univ. Def. Technol.* **26**(5), 39–45 (2004).
11. Y. Zhang et al., "Infrared surface target enhancement based on virtual variational polarization," *Syst. Eng. Electron.* **37**(5), 992–997 (2015).

Yan Zhang is a professor at the ATR Key Laboratory, National University of Defense Technology (NUDT). She received her BS and MS degrees in physics from NUDT in 1997 and 2003, respectively, and her PhD in 2008. She is the author of more than 30 journal papers. Her current research interests include optical image processing. She is a member of SPIE.

Zhi-Guang Shi received his BE degree in automatic control from Shijiazhuang Mechanical Engineering College, Shijiazhuang, China, in 1996 and his ME and PhD degrees in information and telecommunication systems from NUDT, Changsha, China, in 2002 and 2007, respectively. His research interest includes ladar and infrared image processing, radar clutter modeling, and statistical analysis.

Tiao-Wen Qiu received his BE degree in automatic control from Beijing University of Aeronautics and Astronautics, China, in 2011 and his ME degrees in information and telecommunication systems from NUDT, Changsha, China, in 2011 and 2014, respectively. His research interest includes infrared image processing.